



Stability of Graphene on the Si (111) Surface: Insights from Reactive Molecular Dynamics Simulations

Didik Riyanto¹, Edy Kurniawan¹, Husein Muhammad Fras¹, Hanifha Nur Azizah²,
and Rizal Arifin^{2*}

¹Department of Electrical Engineering, Universitas Muhammadiyah Ponorogo, Jl. Budi Utomo No. 10 Ponorogo, Indonesia

²Department of Mechanical Engineering, Universitas Muhammadiyah Ponorogo, Jl. Budi Utomo No. 10 Ponorogo, Indonesia

Abstract: The remarkable characteristics of graphene render it well-suited for a diverse range of applications, particularly in the realm of electronic devices. After the synthesis process, the two-dimensional material known as graphene is then transferred onto a substrate. Silicon (Si) is considered a suitable choice for this purpose. Therefore, it has become essential to investigate the stability of graphene on silicon surfaces. This study utilized reactive molecular dynamics simulations to investigate the thermal stability of graphene on a Si (111) substrate across a temperature range of 300 to 1500 K. The results demonstrate the exceptional stability of graphene on this particular surface. This phenomenon can be explained by the restricted intermolecular interactions between the carbon atoms in graphene and the silicon atoms on the substrate surface. The study findings indicate that graphene exhibits a dome-shaped configuration on the Si (111) surface. In this configuration, only the carbon atoms located at the periphery of the graphene structure interact with the silicon atoms present on the underlying substrate.

Keywords: Graphene, Thermal Stability, Si (111) Surface, Dome-shaped Configuration, Reactive Molecular Dynamics Simulations.

1. INTRODUCTION

The research community has shown significant interest in the two-dimensional material known as graphene [1–5]. Graphene is widely recognized for its exceptional properties, including high electronic conductivity [6], excellent optical transmission [7], and notable mechanical flexibility [8]. These characteristics position graphene as a promising material for potential applications in electronic devices, such as capacitors [9], transistors [10], and photodetectors [11], in the future. The catalytic ability of graphene in the combustion reaction of 1,3,5-trinitroperhydro-1,3,5-triazine has been investigated by Song *et al.* [12]. According to their findings, it has been reported that wrinkled graphene exhibits a higher level of reactivity compared to its flat counterpart [12]. Furthermore, graphene has been employed as a nano-scale composite material in the field of water filtration [13]. The researchers have successfully demonstrated a notable

distinction between the water samples before and after filtration, suggesting that the filtration process is functioning effectively [13].

Graphene can be synthesized through various methods, one of which is chemical vapor deposition (CVD), a widely recognized technique known for its high efficiency and effectiveness. In the process of CVD, graphene is synthesized on metal substrates, including nickel (Ni), copper (Cu), and platinum (Pt). Following this, the graphene is then transferred onto alternative substrates, such as silicon (Si) and silicon dioxide (SiO₂) surfaces [13, 14]. In 2009, a substrate made of polycrystalline Cu foil was utilized for the initial production of a large-area single-layered graphene film. This achievement has served as a catalyst for further investigation into the synthesis of graphene using metal foils and thin films [15]. In addition, the production of graphene can be achieved through deposition of metal films, offering potential advantages. The utilization of

various metallic substrates for growth purposes can result in unique growth patterns, including rare metals beyond Cu and Ni, as well as binary or ternary alloys that are not easily available in foil form. The regulation of carbon content and the ratio of different metals in an alloy can be efficiently achieved through the control of metal film thickness. The aforementioned control mechanism has a direct impact on the deposition process of graphene and subsequently influences the quantity of layers that are formed. Multiple studies have documented that the process of deposition and annealing on particular single-crystal substrates can result in the formation of single-crystal metal films that display a preferred orientation. The carbon atoms located on or within the thin metal film have the ability to diffuse through it and ultimately reach the interface between the film and substrate. This phenomenon enables the direct growth of graphene on the substrate, thereby eliminating the requirement for growth through transfer methods [16]. Furthermore, Tai *et al.* [17] have achieved successful synthesis of graphene directly on a silicon substrate using metal-free ambient-pressure CVD. This method has resulted in the production of atomically flat monolayer or bilayer graphene, as well as concave bilayer and bulging few-layer graphene domains [18].

While Si is commonly used as a substrate for graphene in electronic applications, there is a limited amount of research available on the stability of graphene on Si surfaces. The stability of graphene on a Si (001) surface was examined by Javvaji *et al.* through molecular dynamics (MD) simulations at temperatures of 100, 300, and 900 K [19]. In a separate study, Zhang *et al.* [20] examined the bonding mechanism between graphene and the surface of a silicon substrate by applying a consistent vertical upward exfoliation velocity.

The objective of the current study was to evaluate the stability of graphene on a Si (111) surface using reactive MD simulations. These computations facilitate the examination of the processes involved in the formation and dissociation of C–C and C–Si bonds on the substrate, which have not been thoroughly investigated in previous studies. The changes in the structural composition of graphene were determined through MD simulations conducted at various temperatures ranging from 300 to 1500 K.

2. METHODOLOGY

The calculations were performed using the ReaxFF module of the Amsterdam Modeling Suite 2022 [21–23]. Additionally, we utilized the ReaxFF force field parameters proposed by Soria *et al.* [24] to accurately represent the atomic interactions involving Si–Si, Si–C, and C–C. Figure 1 illustrates the Si (111) substrate comprising of four layers having a total of 600 Si atoms. The lowermost two layers were held in a fixed position to accurately replicate the substrate’s thickness. Furthermore, the structural optimization was enhanced by the introduction of a carbon atom or carbon ring into the substrate. MD simulations were utilized to examine the thermal stability of graphene on the Si (111) surface. The temperature was incrementally increased from 300 to 1500 K in a systematic manner with increments of 100 K. A time step of 0.25×10^{-3} picoseconds was selected along with a temperature increase rate of 8 Kelvin per picosecond. Equilibration was performed at each temperature for a duration of 25 picoseconds. The temperature control in the simulation was achieved by utilizing the Nosé-Hoover thermostat [25–27]. The adsorption energies (E_{ads}) of the C atoms and C rings at different sites on the Si (111) surface were calculated using the following equation:

$$E_{ads} = E_{sc} - (E_s + E_c) \quad (1)$$

where, E_{sc} represents the energy of the system, which includes the Si substrate and the C atom or ring, E_s represents the energy of the substrate, while E_c represents the energy of the isolated C atom or ring. The analysis of the simulation results

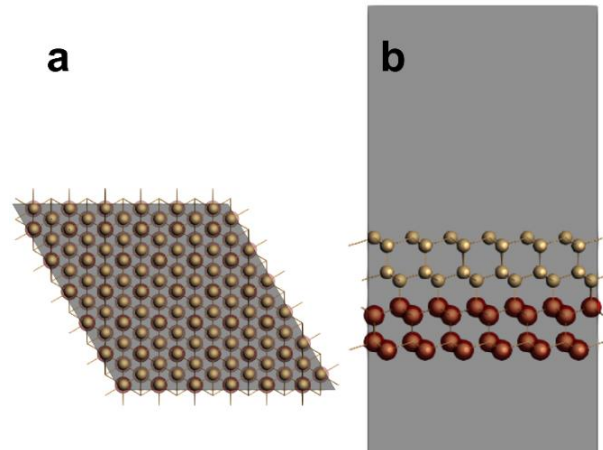


Fig. 1. (a) Top and (b) side views of the initial configuration of the Si (111) substrate. The Si atoms are represented by yellow spheres.

trajectory was conducted using the Ovito software [28]. Furthermore, a coordination analysis was conducted on the C atoms in graphene on the Si (111) surface at various simulation temperatures.

3. RESULTS AND DISCUSSION

The stability of graphene was evaluated through the calculation of adsorption energies for C atoms and hexagonal carbon rings on the Si (111) substrate. Following that, it underwent evaluation via MD simulations, spanning a temperature range from 300 to 1500 K.

3.1 Adsorption Energies of C Atoms and C Rings on the Si (111) Surface

In Table 1, the adsorption energies and heights of the C atoms at different sites on the Si (111) surface are presented. The results indicate that the C atoms located above the Si atoms in the second and third layers occupy the hollow 2 and hollow 3 sites, respectively. According to the data presented in Table 1, it can be observed that the hollow 2 site exhibits the highest adsorption energy (-3.87 eV), while the bridge site demonstrates the lowest adsorption energy (-5.74 eV). The h (Å) data pertains to the vertical distance between the C atoms and the Si (111) surface. The C atoms situated at the bridge site exhibit a vertical displacement of 0.12 Å from the Si (111) surface. Conversely, the C atoms positioned at the hollow 2 site show a greater vertical displacement of 1.66 Å from the substrate.

Table 1. Adsorption energies (E_{ads}) and heights (h) of C atoms at various sites on the Si (111) surface.

Site	E_{ads} (eV)	h (Å)
Top	-4.14	1.38
Bridge	-5.74	0.12
Hollow 2	-3.87	1.66
Hollow 3	-4.75	1.08

Figure 2 illustrates the adsorption sites on the Si (111) surface in relation to the C atoms, as outlined in Table 1. In Figure 2a, it can be observed that the C atoms are positioned directly above the Si atoms in the uppermost layer. The distance between the C atoms and the Si atoms is precisely 1.38 Å. In Figure 2b, it can be observed that the C atoms are positioned between the Si atoms in both the first and second layers. Notably, both sets of Si atoms exhibit a slight displacement from their initial positions, facilitating contact between the C atoms

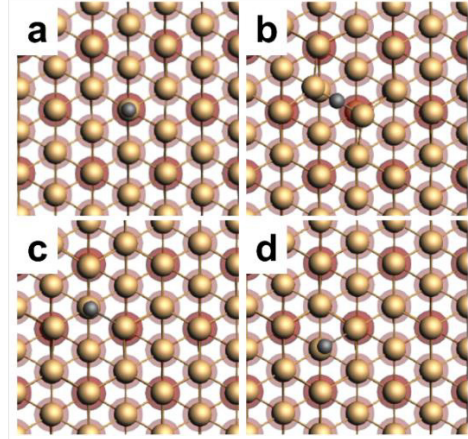


Fig. 2. Optimized arrangement of C atoms on the Si (111) surface at four distinct locations: (a) top site, (b) bridge site, (c) hollow site situated above the second layer of Si atoms, and (d) hollow site situated above the third layer of Si atoms. The Si and C atoms are represented by the yellow and gray spheres, respectively.

and the surface. In comparison to the adsorption energies documented for alternative adsorption sites, this phenomenon yields the most minimal adsorption energy value. The findings of this study align with prior research, which suggests that C atoms adsorbed onto the Si (111) surface exhibit a preference for bridge sites [29]. Figures 2c–d demonstrate that the C atoms adsorbed onto the hollow 2 and hollow 3 sites undergo a subtle displacement towards a Si atom positioned in the top layer. This displacement leads to the establishment of chemical bonds between them.

Table 2 presents the adsorption energies of hexagonal C rings on the Si (111) surface, considering different locations. Sites 1, 2, and 3 correspond to the positions located above the Si atoms in the first, second, and third layers of the substrate, respectively. The adsorption energy of the C ring at site 1 exhibits a positive value, suggesting the presence of a repulsive interaction between the C ring and Si atoms on the substrate surface. This is supported by the observation of a Si atom displacement in the uppermost region of the substrate, resulting in the penetration of the C ring into the substrate (refer to atom 1 in Figure 3a). The adsorption energies of the C rings situated at sites 2 and 3 exhibit negative values, suggesting the presence of attractive interactions between the C and Si atoms on the surface of the Si (111) substrate. The site with the lowest adsorption energy is designated as site 3. At this location, each C atom in the C ring establishes a binding interaction with the

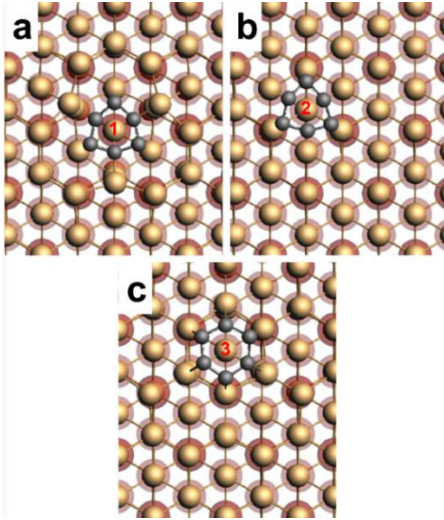


Fig. 3. Optimized arrangement of C rings on the Si (111) surface at three distinct locations: the sites situated above the (a) first, (b) second, and (c) third layers of Si atoms. The Si and C atoms are represented as yellow and gray spheres, respectively. The spheres denoted by indices 1, 2, and 3 correspond to the Si atoms located in the first, second, and third layers, respectively.

Si atoms found in both the first and second layers (refer to Figure 3c). The hexagonal shape of the C ring is preserved in this scenario. At location 3, it is evident that specific C atoms are unable to form bonds with Si atoms in the third layer due to the considerable distance separating them. Only the C atoms that are in close proximity to the Si atoms in the first layer have the capability to establish chemical bonds. This phenomenon is accountable for the distortion of the C ring. Based on the results obtained, it can be concluded that the adsorption of the C ring is more favorable at site 3 on the Si (111) surface.

Table 2. Adsorption energies (E_{ads}) of C rings at various sites on the Si (111) surface. The positions above the Si atoms in the first, second, and third layers of the substrate are represented by sites 1, 2, and 3, respectively.

Adsorption Site	E_{ads} (eV)
Site 1	1.94
Site 2	-3.88
Site 3	-4.00

3.2 Effect of Temperature on Graphene Stability on Si (111) Surface

The graph in Figure 4 illustrates the variation in the maximum height of a C atom in graphene in relation to the Si (111) surface at different temperatures.

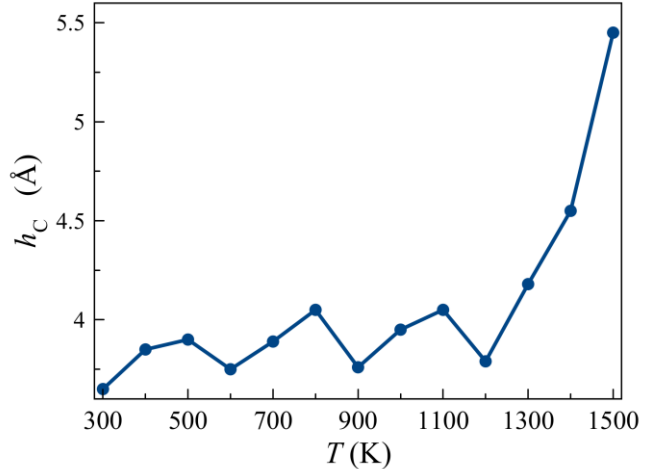


Fig. 4. The maximum vertical distance (h_c) between a C atom in graphene and the Si (111) surface at temperatures of 300 to 1500 K.

The maximum height exhibits slight variations within the temperature range of 300 to 1200 K, but undergoes a notable increase between 1300 and 1500 K. Figure 5 illustrates the dome-shaped morphology of graphene observed on the Si (111) surface. It is worth mentioning that the C atoms located at the periphery of the graphene structure establish chemical bonds with the Si atoms present on the surface of the substrate. Conversely, the C atoms situated in the central region of the graphene structure exhibit a tendency to distance themselves from the Si (111) surface. Figures 5a–b depict the similarity observed in the graphene domes on the Si (111) surface at temperatures of 300 and 900 K, respectively. Additionally, Figure 5c illustrates the alterations in the shape of the graphene dome when subjected to a temperature of 1500 K.

Furthermore, the determination of the graphene structure can be achieved through the analysis of the radial distribution function $g(r)$, as depicted in Figure 6. The $g_{C-C}(r)$ plots, which illustrate the interatomic distances between C atoms in graphene, demonstrate a significant resemblance across the temperature range from 300 to 1500 K. The primary peak of $g_{C-C}(r)$ is observed within the range of 1.42 to 1.47 Å between carbon-carbon (C-C) atoms. The discrepancy in the observed value can be attributed to the vibrational freedom of C atoms at higher temperatures. The obtained value aligns with the results of prior research, which suggest that the distance between C-C atoms in graphene falls within the range of 1.42 Å to 1.49 Å [30-31]. The obtained results demonstrate the remarkable stability of graphene on the Si (111) surface, where

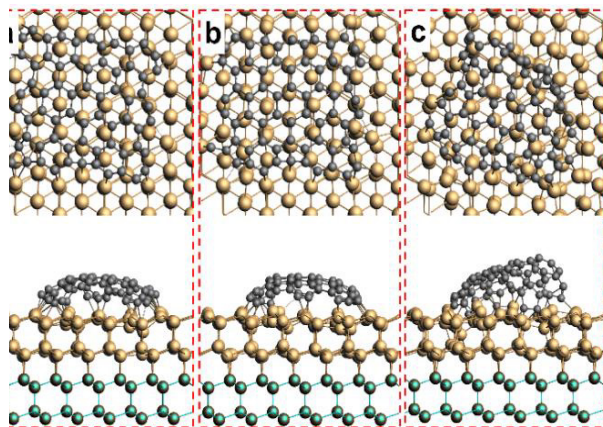


Fig. 5. Graphene on the Si (111) surface at temperatures of (a) 300 K, (b) 900 K, and (c) 1500 K. The upper and lower images depict perspectives from the top and side, respectively.

the interactions between the C atoms in graphene and the Si atoms on the substrate surface are found to be minimal, thus playing a significant role in this aspect. The results obtained are consistent with the findings of previous studies conducted by Zhang *et al.* [20] and suggest that a vertical upward velocity of 4.3 Å/ps is necessary for the exfoliation of monolayer graphene from the Si surface.

4. CONCLUSION

The stability of graphene on a Si (111) surface was investigated through the utilization of reactive MD simulations. The Si (111) bridge site demonstrated a higher affinity for the adsorption of C atoms compared to other potential sites, such as the top and hollow sites. Additionally, it was observed that the C ring predominantly occupies the surface site positioned directly above the Si atoms in the third layer. Furthermore, the findings of this investigation suggest that graphene demonstrates remarkable stability on the Si (111) surface at temperatures up to 1500 K. This stability can be attributed to the limited interactions between the C atoms in graphene and the Si atoms in the substrate.

5. ACKNOWLEDGMENTS

The research conducted in this study received financial support from Universitas Muhammadiyah Ponorogo through a grant for fundamental research in 2023. The grant was awarded under contract #066/VI.4/PN/2023.

6. CONFLICT OF INTEREST

The authors declare no conflict of interest.

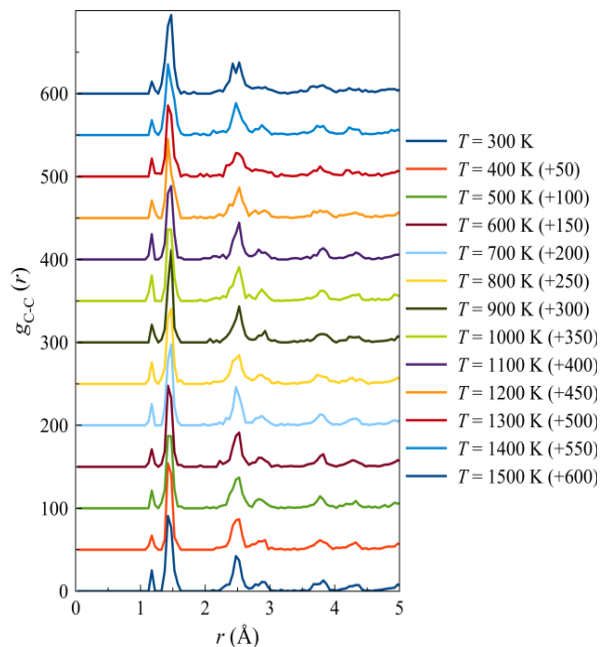


Fig. 6. Radial distribution functions of C–C interatomic distances, $g_{C-C}(r)$, in graphene on the Si (111) surface over the temperature range of 300 to 1500 K.

7. REFERENCES

1. Y. Liu, M. Xu, X. Zhu, M. Xie, Y. Su, N. Hu, Z. Yang, and Y. Zhang. Synthesis of carbon nanotubes on graphene quantum dot surface by catalyst free chemical vapor deposition. *Carbon* 68: 399–405 (2014).
2. R. Arifin, Y. Shibuta, K. Shimamura, and F. Shimojo. First principles molecular dynamics simulation of graphene growth on Nickel (111) surface. *IOP Conference Series: Materials Science and Engineering* 128: 012032 (2016).
3. R. Arifin, Y. Shibuta, K. Shimamura, F. Shimojo, and S. Yamaguchi. Ab Initio Molecular Dynamics Simulation of Ethylene Reaction on Nickel (111) Surface. *Journal of Physical Chemistry C* 119: 3210–3216 (2015).
4. R. Arifin, Y. Shibuta, K. Shimamura, and F. Shimojo. First principles calculation of CH₄ decomposition on nickel (111) surface. *The European Physical Journal B* 88: 303 (2015).
5. Y. Shibuta, R. Arifin, K. Shimamura, T. Oguri, F. Shimojo, and S. Yamaguchi. Ab initio molecular dynamics simulation of dissociation of methane on nickel(111) surface: Unravelling initial stage of graphene growth via a CVD technique. *Chemical Physics Letters* 565: 92–97 (2013).
6. K.S. Novoselov, A.K. Geim, S.V. Morozov, D. Jiang, Y.Zhang, S.V. Dubonos, I.V. Grigorieva and A.A. Firsov. Electric Field Effect in Atomically Thin Carbon Film. *Science* 306: 666–669 (2004).

7. R.R. Nair, P. Blake, A.N. Grigorenko, K.S. Novoselov, T. J. Booth, T. Stauber, N.M.R. Peres and A.K. Geim. Fine Structure Constant Defines Visual Transparency of Graphene. *Science* 320: 1308–1308 (2008).
8. A. K. Geim, K. S. Novoselov. The rise of graphene. *Nature Materials* 6: 183–191 (2007).
9. S.H. Abro, F.Hussain, M.Sohail, D.Tariq, K. Jawed, R. Sanwal, and M.N. Alghamdi. Development and Synthesis of Composite Electrode (rGO/G/PANI) for Capacitor from Burnout Battery Powder: Composite Electrode (rGO/G/PANI) for Capacitor. *Proceedings of the Pakistan Academy of Sciences: A* 57: 41–50 (2021).
10. A.Béraud, M.Sauvage, C.M. Bazan, M. Tie, A. Bencherif, and D. Bouilly. Graphene field-effect transistors as bioanalytical sensors: design, operation and performance. *Analyst* 146: 403–428 (2021).
11. K. Murali, N. Abraham, S. Das, S. Kallatt, and K. Majumdar. Highly Sensitive, Fast Graphene Photodetector with Responsivity >106 A/W Using a Floating Quantum Well Gate. *ACS Applied Materials & Interfaces* 11: 30010–30018 (2019).
12. L. Song, F.Q. Zhao, S.Y. Xu, X.H. Ju, and C.C. Ye. Onset of catalytic activity of graphene nanosheets in reaction with energetic materials evaluated by ReaxFF molecular dynamics simulation. *Surfaces and Interfaces* 31: 102024 (2022).
13. S.H. Abro, A. Chandio, I.A. Channa, and A.S. Alaboodi. Design, Development and Characterization of Graphene Sand Nano-Composite for Water Filtration. *Pakistan Journal of Scientific and Industrial Research Series A: Physical Sciences* 63A: 118–122 (2020).
14. D.V. Smovzh, I.A. Kostogrud, E.V. Boyko, and M.A. Morozova. Graphene transfer from a copper surface to a silicon substrate. *Journal of Physics: Conference Series* 1675: 012098 (2020).
15. Z. Khanam, I. Riaz, A. Rasheed, and R. Jalil. Fabrication and Identification of Graphene Layers on Silicon Dioxide and Flexible PMMA Substrates: Graphene fabrication. *Proceedings of the Pakistan Academy of Sciences: A* 53: 431–445 (2021).
16. X. Li, W. Cai, J. An, S. Kim, J. Nah, D. Yang, R. Piner, A. Velamakanni, I. Jung, E. Tutuc, S.K. Banerjee, L. Colombo, and R.S. Ruoff. Large-Area Synthesis of High-Quality and Uniform Graphene Films on Copper Foils. *Science* 324: 1312–1314 (2009).
17. S. Xu, L. Zhang, B. Wang, and R.S. Ruoff. Chemical vapor deposition of graphene on thin-metal films. *Cell Reports Physical Science* 2: 100372 (2021).
18. L. Tai, D. Zhu, X. Liu, T. Yang, L. Wang, R. Wang, S. Jiang, Z. Chen, Z. Xu, and X. Li. Direct Growth of Graphene on Silicon by Metal-Free Chemical Vapor Deposition. *Nano-Micro Letters* 10: 20 (2017).
19. B. Javvaji, B.M. Shenoy, D.R. Mahapatra, A. Ravikumar, G.M. Hegde, and M.R. Rizwan. Stable configurations of graphene on silicon. *Applied Surface Science* 414: 25–33 (2017).
20. Q. Zhang, Y. Zhao, X. Ma, Y. Zhao, X. Pang. Study on bonding mechanism of graphene on silicon substrate. *Modern Physics Letters B* 32: 1850265 (2018).
21. A.C.T. van Duin, W.A. Goddard, M.M. Islam, H. van Schoot, T. Trnka, and A.L. Yakovlev. ReaxFF 2022.1 (2022) <http://www.scm.com> (accessed 22 January 2023)
22. A.C.T. van Duin, S. Dasgupta, F. Lorant, and W.A. Goddard. ReaxFF: A reactive force field for hydrocarbons. *Journal of Physical Chemistry A* 105: 9396–9409 (2001).
23. K. Chenoweth, A.C.T. van Duin, and W.A. Goddard. ReaxFF reactive force field for molecular dynamics simulations of hydrocarbon oxidation. *Journal of Physical Chemistry A* 112: 1040–1053 (2008).
24. F.A. Soria, W. Zhang, P.A. Paredes-Olivera, A.C.T. van Duin, and E.M. Patrito. Si/C/H ReaxFF Reactive Potential for Silicon Surfaces Grafted with Organic Molecules. *Journal of Physical Chemistry C* 122: 23515–23527 (2018).
25. S. Nosé. A molecular dynamics method for simulations in the canonical ensemble. *Molecular Physics* 52: 255–268 (1984).
26. S. Nosé. A unified formulation of the constant temperature molecular dynamics methods. *The Journal of Chemical Physics* 81: 511–519 (1984).
27. W.G. Hoover. Canonical dynamics: Equilibrium phase-space distributions. *Physical Review A* 31: 1695 (1985).
28. A. Stukowski. Visualization and analysis of atomistic simulation data with OVITO—the Open Visualization Tool. *Modelling and Simulation in Materials Science and Engineering* 18: 015012 (2010).
29. T. Takai, T. Halicioğlu, and W.A. Tiller. Adsorption, potential maps and diffusion of Si, C, and SiC on A Si(111) surface. *Surface Science* 164: 327–340 (1985).
30. A.Z. Alzahrani. Structural and Electronic Properties of Graphene upon Molecular Adsorption: DFT Comparative Analysis. In: Graphene Simulation. J.R. Gong (ed.). *IntechOpen, Rijeka, Croatia*, pp. 21–38 (2011).
31. M. Igami, S. Okada, and K. Nakada. Electronic and geometric structures of fluorine adsorbed graphene. *Synthetic Metals* 121: 1233–1234 (2001)